Journal of Sol-Gel Science and Technology (2022) 104:606–616
https://doi.org/10.1007/s10971-022-05814-z

INVITED PAPER: SOL-GEL AND HYBRID MATERIALS FOR BIOLOGICAL AND HEALTH (MEDICAL) APPLICATIONS

Effects of the silicon-containing chemical species dissolved from chitosan–siloxane hybrids on nerve cells

Kosei Hattori[1] · Satoshi Hayakawa[2] · Yuki Shirosaki[1]

Received: 27 February 2022 / Accepted: 11 April 2022 / Published online: 7 May 2022

Abstract

Silicic acid components from bioactive glass activate osteoblasts gene for bone generation. Many studies have been reported on osteoblast compatibility and bone regeneration using composites and hybrids, including silica or siloxane units. We previously synthesized chitosan−siloxane hybrids via a sol-gel method and observed bone and nerve regeneration. However, it is not clear the structure of molecules involving silicon atoms that has a more effective role in the cell activity and their mechanisms of cell activation. In this study, we prepared hybrid materials from chitosan and different types of alkoxysilane, 3-glycidoxypropyltrimethoxysilane (GPTMS), 3-glycidoxypropyldimethoxymethylsilane (GPDMS), and tetraethoxysilane (TEOS), and investigated the structures of the silicon-containing species dissolved from each hybrid and their effect on the proliferation of nerve cells. The silicon-containing species in the extraction were mainly 100–600 molecular weight, indicating they were chitin/chitosan units and monomeric hydrolyzed GPTMS, GPDMS, and TEOS. The nerve cell proliferation was inhibited by the chitosan–GPTMS and GPDMS hybrid extractions. The silicon-containing species were not taken up by the cells. The silicon-containing species dissolved from the hybrids were adsorbed to the cells or they inactivated biomolecules in the culture medium, suppressing cell proliferation.

Graphical abstract

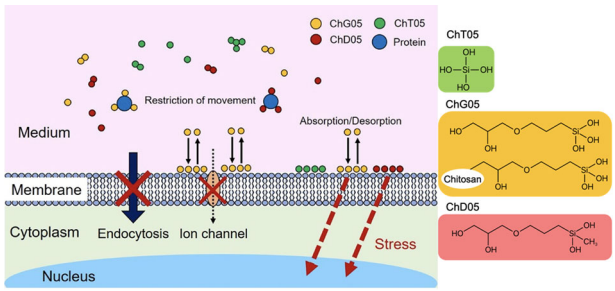

Keywords chitosan-siloxane hybrid · silicon-containing species · nerve cell · cell proliferation

These authors contributed equally: Kosei Hattori, Satoshi Hayakawa

✉ Yuki Shirosaki
yukis@che.kyutech.ac.jp

[1] Faculty of Engineering, Kyushu Institute of Technology, 1-1 Sensuicho, Tobata-ku, Kitakyushu 804-8550 Fukuoka, Japan

[2] Faculty of Interdisciplinary Science and Engineering in Health Systems, Okayama University, 3-1-1 Tsushima-naka, Kita-ku, Okayama 700-8530, Japan

Highlights

- The silicon-containing species dissolved from chitosan–siloxane hybrid were corresponding to hydrolyzed GPTMS, GPDMS, and TEOS with chitosan oligomers.
- Nerve cells did not uptake the silicon-containing species.
- The silicon-containing species derived from Chitosan–GPTMS and –GPDMS hybrids inhibited nerve cell proliferation.
- The silicon-containing species derive the hybrids adsorbed to the cell surface or inactivated biomolecules in the medium.

1 Introduction

Silicon is an essential trace element in the human body and is especially in connective tissues as well as skin, bone, tendon, liver, heart, and muscles [1]. Carlisle revealed that silicon is required for ossification in rats and chicks [2]. Hench et al. reported that the silicate component derived from bioglass activates the genes of osteoblast cells and promotes bone regeneration [3, 4] according to the concentration of Si(IV). For example, human osteoblast cell differentiation was promoted when the concentration of silicic acid eluted from Bioglass® 45S5 was 0.59 mM [3]. When 8.19 mM of silicon was eluted from foamed 57 S bioactive glass, 50% apoptosis occurred in human osteoblast cells [4]. In addition, Shie et al. [5] found that the 4 mM silicon leached from calcium silicate cement increased MG63 cell proliferation, differentiation, and mineralization, while 6 mM suppressed proliferation and differentiation, and increased the number of apoptotic cells. Orthosilicic acid is believed to be taken up by bone cells through sodium−bicarbonate ion channels [6], and mesenchymal stem cells can take up silica nanoparticles (50–120 nm) by endocytosis [7]. However, there is little research regarding the effect of silicon on other cells. For example, human skin fibroblasts have high cell viability when the concentration of orthosilicic acid derived from mesoporous silica nanoparticles and soluble silicic acid is 100 µM [8]. Quignard et al. determined that silica nanoparticles (particle size 12–500 nm) at concentrations of 10–50 µg/mL were less likely to be taken up by human colon cancer cells when the particle size is larger [9]. Bonazza et al. reported that endothelial cell proliferation was enhanced, and osteoblasts and fibroblasts increased their expression of collagen Type I in the medium containing 0.5 mM or 1 mM sodium orthosilicic acid [10]. Recently, our group focused on the effect of the silicon structures on cells. Shirosaki et al. prepared the chitosan−siloxane hybrids with 3-glycidoxypropyltrimethoxysilane (GPTMS) and tetraethoxysilane (TEOS) [11]. The osteoblastic cell proliferation was different between the hybrid, even with the same Si (IV) concentration released into the culture medium, which suggests that the differences in molecular structure of the species involving silicon atoms or the molecular weight of the silicon-containing species dissolved from the hybrids in the culture medium also affect the behavior.

The basic units of the peripheral nerve are the nerve fiber and Schwann cells. The peripheral nerve comprises a myelin sheath and Schwann sheath around the axon extending from the nerve cell in the spinal cord and spinal nerves [12]. Peripheral nerves may be severed in cases of trauma such as traffic accidents, disasters, or common surgeries. Although 200,000 nerve regeneration surgeries are performed annually worldwide, only 25%, 3%, and 10% of them restore motor function, sensation, and axons to the target organ, respectively [13]. In addition, the quality of life of patients with peripheral nerve injuries is diminished [14]. Therefore, nerve repair is one of the major challenges faced by clinicians [15]. Chitosan-based materials are used as nerve conduits because of their mechanical property and slow biodegradability. Basically, the chitosan-based nerve conduits are modified with other biodegradable polymers to improve the hydrophilicity and the elasticity, etc. [16–18]. In our laboratory, we also applied the chitosan–GPTMS hybrids to nerve regeneration [19–22]. Chitosan is a biopolymer that is non-toxic, biocompatible, and biodegradable. The degradation rate, mechanical properties, and biocompatibility can be modified by the introduction of the siloxane network. When chitosan–GPTMS hybrids were introduced into sciatic nerve defects in rats, the porous hybrid promoted the recovery of nerve function and improved the recovery rate of sensory and motor functions more than the solid hybrid [19]. Unfortunately, we have not explained yet why the results are different between the porous and the solid hybrids. Moreover, the effect of the dissolved silicon-containing species on the nerve cells is still unclear. In this study, we focused on why the solid membranes did not improve the nerve regeneration with respect to the molecular structures of the silicon-containing species dissolved from the hybrids in the medium. GPTMS, TEOS, and 3-glycidoxypropyl dimethoxymethylsilane (GPDMS) were used to prepare the solid membranes (Fig. 1).

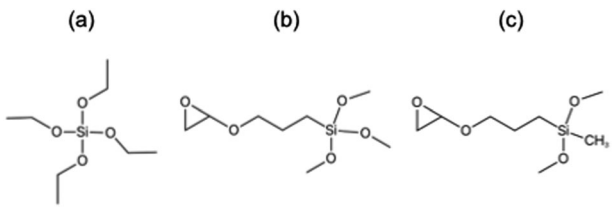

Fig. 1 The structure of alkoxysilane. **a** TEOS, (**b**) GPTMS, (**c**) GPDMS

Table 1 Starting composition of chitosan–siloxane hybrid (molar ratio)

	Chitosan	TEOS	GPTMS	GPDMS	HOAc
ChT05	1	0.5	–	–	3.5
ChG05	1	–	0.5	–	3.5
ChD05	1	–	–	0.5	3.5

The effect of the molecular structures of the dissolved silicon-containing species on nerve cells were examined.

2 Experimental section

2.1 Preparation of the chitosan–siloxane hybrid membranes

Chitosan–siloxane hybrids were prepared according to a previous report [11]. Chitosan (high molecular weight, 310,000–371,000, DA > 75%, Sigma-Aldrich®, St. Louis, MO, USA) was dissolved in an aqueous 0.25 M acetic acid (HOAc) solution to yield a concentration of 2.0 mass% using a planetary centrifuge (ARE-310, Thinky, Tokyo, Japan) at 2000 rpm (Program: MIX 5 min−DEFOAM 3 min) ×3, MIX 5 min). An appropriate volume of TEOS (Alfa Aesar, Ward Hill, MA, USA), GPDMS (Shinetsu Chemical Industry, Tokyo, Japan), and GPTMS (Alfa Aesar) were hydrolyzed by adding 10 mL of a 0.25 M HOAc solution and stirred at room temperature for 6, 5, and 1 h, respectively; the solutions were then added to the chitosan solution. The resulting solutions were mixed by a planetary centrifuge with the same program used for the chitosan solutions. The solutions were poured into polypropylene containers and stood overnight at room temperature. The solutions were then incubated at 60 °C for gelation in a sealed container. And then the gels were dried at 60 °C to yield the hybrid membranes with the lid open. The hybrid membranes were soaked in a 0.2 M sodium hydroxide aqueous solution to neutralize the remaining acetic acid, washed with distilled water, and dried at 60 °C for 3 h. Table 1 indicates the starting compositions of the precursor solutions for the hybrid membranes and the sample name. The hybrid membranes were cut into a circle (diameter 6 mm) and sterilized by ethylene oxide gas (20% CAPOX, 45 °C, 50% humidity, Steri-Tech Inc., Saitama, Japan).

2.2 Structural characterization of the hybrid membranes

Solid-state NMR measurements were performed using an Agilent DD2 500 MHz NMR spectrometer (Agilent Technologies, Inc., Santa Clara, CA, USA) operating at 11.7 Tesla. A zirconia rotor with a diameter of 3.2 mm was used with an Agilent HXY T3 MAS probe. The rotor spinning frequency for magic angle spinning (MAS) was 15 kHz. $^{1}H \rightarrow {}^{13}C$ cross-polarization (CP)-MAS NMR experiments were operated at resonance frequencies of 499.76 MHz and 125.66 MHz for ^{1}H and ^{13}C, respectively, using a 2.3 µs pulse length (π/2-pulse angle) for ^{1}H, 500 µs contact time, and 10 s recycle delays. The signals from 8360 to 25,630 pulses were accumulated for each film, with adamantane ($C_{10}H_{16}$) as the external reference (38.52 ppm vs. 0 ppm TMS). $^{1}H \rightarrow {}^{29}Si$ CP-MAS NMR experiments were performed at resonance frequencies of 499.76 MHz and 99.28 MHz for ^{1}H and ^{29}Si, respectively, using a 3.6 µs pulse length (π/2-pulse angle) for ^{1}H, 5 ms contact time, and 5 s recycle delays. The signals from 20,230 to 88,005 pulses were accumulated for each film, with polydimethylsilane (PDMS) as the external reference (−34.44 ppm vs. 0 ppm TMS).

2.3 Preparation and characterization of the hybrid membranes extractions

Circle membranes were soaked in 0.1 mL of ultrapure water per membrane (Life Technologies, Carlsbad, CA, USA) at 37 °C for 1 week. Extractions were filtrated using a syringe filter (pore size 0.22 µm, TPP, Trasadingen, Schaffhausen, Switzerland). The amount of Si(IV) released into the extractions was measured by inductively coupled plasma emission spectrometry (ICP, ICPS-8000, Shimazu Corporation, Kyoto, Japan). The molecular weight of the species released into the extractions was determined by electron spray ionization time of flight mass spectrometry (TOF-MS, JMS-T100LP, JEOL, Tokyo, Japan). The extractions were analyzed in negative mode under the following experimental conditions: the desolvating chamber and orifice temperatures were 250 °C and 80 °C, respectively; the voltages of the orifices and ion guide RF were 85 V, 25 V, and 1 kV, respectively. Spectra were collected throughout an *m/z* range from 0 to 1000.

2.4 Biological assessment

2.4.1 Preparation of medium containing Si(IV) and cell culture

The extractions were diluted with ultrapure distilled water (Life Technologies) to 5 µM of silicon concentration and sterilized using a syringe filter (pore size 0.22 µm, TPP). Dulbecco's modified Eagle's medium (D-MEM) and sodium hydrogen carbonate were added to the extractions. RT4-D6P2T rat Schwann cells were cultured in the medium with 10% fetal bovine serum (FBS), 2 mM L-glutamine, and 100 U/mL penicillin-streptomycin for 1, 3, and 5 days for cell proliferation and morphology observations.

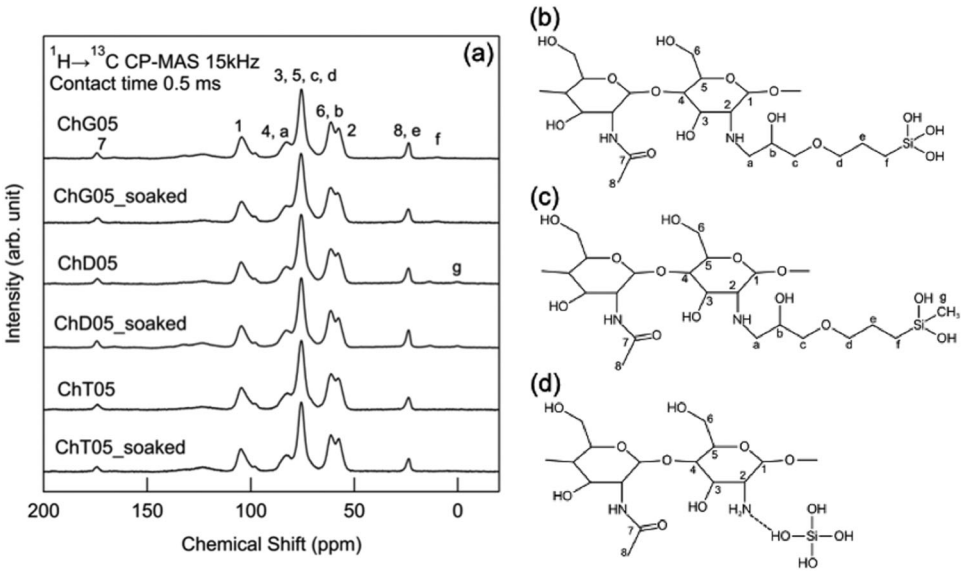

Fig. 2 **a** ^{13}C CP-MAS NMR spectra of the hybrids before and after soaking in ultrapure water at 37 °C for 1-week and the estimated molecular structure of (**b**) ChG05, (**c**) ChD05, and (**d**) ChT05

2.4.2 Cell proliferation

MTT assay was used to estimate the cell viability and proliferation [23]. After culture, the cells were incubated with 5 mg/mL MTT at 37 °C for 4 h. After incubation, the culture medium was removed and the formazan salts were dissolved with dimethyl sulfoxide. The absorbance was measured at 560 nm.

2.4.3 Cell morphology

After culture, the medium was removed, the cells on the plates were rinsed with PBS (Thermo Fisher Scientific, Waltham, MA, USA) and fixed by a 4% paraformaldehyde solution (FUJIFILM Wako Pure Chemical Corporation, Osaka, Japan). Cells were washed with PBS and covered with a 0.1% Triton X-100/PBS solution and then washed twice with a 0.05% Tween® 20/PBS solution (washing solution). The actin filament was stained with Phalloidin Alexa Fluor® 488 (LONZA, Basel, Basel-Stadt, Switzerland) and the surface was washed twice with the washing solution. The nuclei were stained by 4′, 6-diamino-2-phenylindol (DAPI, Invitrogen, Waltham, MA, USA) and washed twice with the washing solution. The cell morphologies were observed by an inverted fluorescence microscope (IX73, filter DAPI: U-FUNA, Phalloidin: U-FBW, OLYMPUS, Tokyo, Japan) and imaged.

2.4.4 Nerve cell uptake of Si(IV) released from hybrids

The medium was collected after 5 days of culture. The number of cells were counted and dissolved by 1 M nitric acid for cell lysis. The collected medium and cell lysis were filtered through a 0.2 µm filter, and their Si(IV) concentration was measured by ICP spectrometry.

2.5 Statistical analysis

The viability results were analyzed using one-way analysis of variance (ANOVA) followed by Tukey's test with a significance level of $p < 0.01$.

3 Results and discussion

3.1 Characterization of hybrids and extractions

Figure 2 shows the ^{13}C CP-MAS NMR spectra of the hybrids before and after soaking in ultrapure water. Chitosan matrix signals appeared at 104.0 (C_1), 82.6 (C_4), 75.6 (C_3 and C_5), 61.4 (C_6), 57.1 (C_2), 174.2 (N-acetyl C=O signal), and 23.9 (N-acetyl-methyl CH_3 signal) ppm in all samples [24, 25]. Cx denote the carbon atoms in Fig. 2b–d. GPTMS-derived signals appeared at 9.9 (C_f), 23.9 (C_e), 61.4 (C_b), 75.6 (C_c and C_d), and 82.6 (C_a) ppm [24]. GPDMS-derived signals appeared at 0.2 (C_g), 13.5 (C_f), 23.9 (C_e), 61.4 (C_b), 75.6 (C_c and C_d), and 82.6 (C_a) ppm [25]. The carbon of methoxy and ethoxy groups were not detected in the spectra of any sample, indicating that the alkoxy groups were completely hydrolyzed. In addition, the carbon of the epoxy group of GPTMS and GPDMS was not detected 42.9 and 49.8 ppm [26] in the spectra of ChG05 and ChD05 (Table 1), which means the epoxy group reacted to the amino group of chitosan or opened. The peak of C_2 changes because of the reaction between the epoxy group and amino group [27]. The intensities of C_2/C_1 in the

ChG05 and ChD05 spectra before soaking were 0.52 and 0.46. After soaking, the intensities of C_2/C_1 in the ChG05 and ChD05 spectra were 0.42 and 0.54, and nearly the same before and after immersion in water. Therefore, the bonding between epoxy groups of the alkoxysilane and amino groups of chitosan did not break and the degradation of the hybrids in water occurred by hydrolysis of the glycosidic bond.

Figure 3 shows the ^{29}Si CP-MAS NMR spectra demonstrating the change of the methoxysilane or ethoxysilane groups of GPTMS, GPDMS, and TEOS in the hybrids before and after soaking in ultrapure water. The profiles were deconvoluted into some component peaks due to T^0, T^1, T^2, and T^3 siloxane units in ChG05, D^0, D^1, and D^2 in ChD05, and Q^2, Q^3, and Q^4 in ChT05 [28–30]. T^0, T^1, T^2, and T^3 denoted R–Si (–OCH_3, $OH)_3$, R–Si(–OSi) (OCH_3, $OH)_2$, R–Si(–$OSi)_2$ (OCH_3, OH), and R−Si(–$OSi)_3$ (R is the organic skeleton derived from GPTMS), D^0, D^1, and D^2 denote R−Si(–OCH_3, $OH)_2$ (–CH_3), R−Si(–OSi) (OCH_3, OH) (–CH_3), and R−Si(–$OSi)_2$ (–CH_3) (R is the organic skeleton derived from GPDMS), and Q^2, Q^3, and Q^4 denote Si(–$OSi)_2$ $(OH)_2$, Si(–$OSi)_3$ (OH), Si(–$OSi)_4$, respectively.

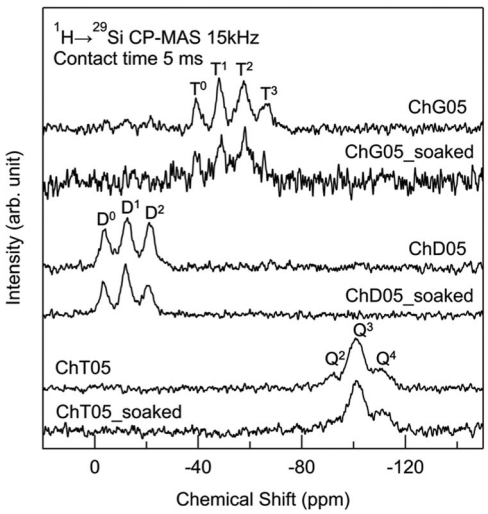

Fig. 3 ^{29}Si CP-MAS NMR spectra of the hybrids before and after soaking in ultrapure water at 37 °C for 1 week

Tables 2 and 3 show the chemical shift (δ), full width at half-maximum (FWHM), relative peak area (%) of each unit, and the number of Si–O–Si bridging bonds per Si atom (N_{bo}/Si). N_{bo}/Si was derived by condensation of the Si–OH or Si–OCH_3 groups at the silane end of a GPTMS or GPDMS molecule. and it was calculated by Eqs. 1 and 2 according to a simple valence theory [28].

$$\frac{N_{bo}}{Si} = \left(\text{fraction of } T^1\right)\times 1 + \left(\text{fraction of } T^2\right) \times 2 + \left(\text{fraction of } T^3\right) \quad (1)$$

$$\frac{N_{bo}}{Si} = \left(\text{fraction of } D^1\right) \times 1 + \left(\text{fraction of } D^2\right) \times 2 \quad (2)$$

The N_{bo}/Si of both ChG05 and ChD05 decreased from 1.67 to 1.49, and from 1.31 to 1.05 during soaking, respectively, which indicates the siloxane bonds were hydrolyzed in water. In the case of ChT05, Q^4, Q^3, and Q^2

Table 2 ^{29}Si chemical shift (δ (ppm)), full width at half maximum (FWHM (ppm)), and relative area (I (%)) for T unit derived from the ^{29}Si CP-MAS NMR spectra of ChG05

	T^0			T^1			T^2			T^3			N_{bo}/Si
	δ[a]	FWHM[b]	I[c]	δ[a]	FWHM[b]	I[c]	δ[a]	FWHM[b]	I[c]	δ[a]	FWHM[b]	I[c]	
ChG05	−39.58	3.2	13.9	−48.35	3.4	25.8	−57.42	5.7	39.5	−66.16	5.2	20.83	1.67
ChG05_soaked	−39.40	2.5	12.0	−48.76	4.5	30.8	−58.02	6.6	50.4	−65.49	1.1	5.87	1.49

[a]Estimated error of chemical shifts < ±0.05 ppm

[b]Estimated error of FWHM < ±0.1 ppm

[c]Estimated error of relative peak area < ±0.5%

Table 3 ^{29}Si Chemical shift (δ (ppm)), full width at half maximum (FWHM (ppm)), and relative area (I (%)) for D unit derived from the ^{29}Si CP-MAS NMR spectra of ChD05

	D^0			D^1			D^2			N_{bo}/Si
	δ[a]	FWHM[b]	I[c]	δ[a]	FWHM[b]	I[c]	δ[a]	FWHM[b]	I[c]	
ChD05	−4.22	4.7	15.0	−12.81	5.3	38.8	−21.32	4.7	46.2	1.31
ChD05_soaked	−3.58	4.2	25.5	−12.08	4.6	43.9	−20.46	5.3	30.6	1.05

[a]Estimated error of chemical shifts < ±0.04 ppm

[b]Estimated error of FWHM < ±0.1 ppm

[c]Estimated error of relative peak area < ±0.3%

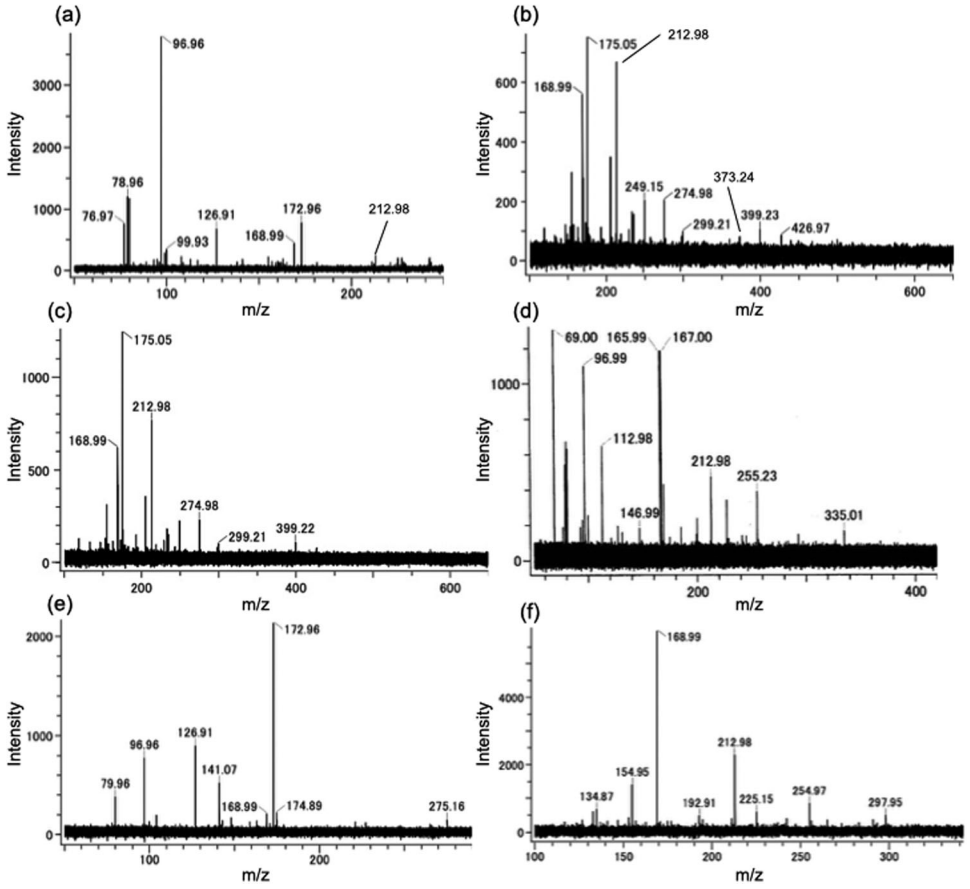

Fig. 4 ESI TOF-MS spectra of the extraction and solution. **a** Ch, (**b**) ChG05, (**c**) ChD05, (**d**) ChT05, (**e**) D-glucosamine, and (**f**) N-acetyl-D-glucosamine

were detected before soaking in water and Q^2 was not detected after soaking. The silicon-containing species derived from ChT05 was eluted by the hydrolysis of the Si–O–Si bonding.

Figure 4 shows the ESI TOF-MS spectra of extractions from Ch (a), ChG05 (b), ChD05 (c), and ChT05 (d), and the aqueous solution of D-glucosamine (e) and N-acetyl-D-glucosamine (f). The structures estimated from the MS spectra are shown in Fig. 5. ESI TOF-MS is excellent for detecting molecules smaller than 550 Da, but not for molecules larger than 4000 Da [31]. The molecular weights of the species in the extractions were 100–400, regardless of the hybrids. The peaks at *m/z* 168.99 and 212.98 are corresponding to one glucosamine unit and one acetyl glucosamine unit by hydrolysis of chitosan chains. The peak at *m/z* 175.05 was detected in ChG05 and ChD05 extractions and the peaks at *m/z* 69.00 and 96.99 were detected in ChT05. These species were attributed to the monomeric compound from the hydrolyzed alkoxysilane. In addition, oligomers of hydrolyzed alkoxysilane were detected in each extraction. The peaks at *m/z* 399.23 and 399.22 in ChG05 and ChD05 were dimers of hydrolyzed GPTMS or GPDMS, and the peak at *m/z* 335.01 was a tetramer of orthosilicate. In the spectrum of ChG05, a peak at *m/z* 373.24 was detected and assigned to one unit of chitosan bound to hydrolyzed GPTMS, which suggests that most of the released species were one unit of chitosan or chitin with a monomeric compound from hydrolyzed GPTMS by hydrolysis of the glycosidic bond of chitosan chains. However, ^{29}Si CP-MAS NMR showed that the T^0 unit was in ChG05; the only monomeric compound derived from GPTMS was also eluted in the extraction of ChG05. The associated peaks were a chitosan-mono-like compound in the TOF-MS spectra of ChD05 and ChT05, suggesting that the amino group of the chitosan interacts with the hydrolyzed GPDMS and TEOS without strong bonding.

3.2 Cell proliferation and morphology with the silicon-containing species

Figure 6 shows the cell proliferation of RT4 nerve cells cultured in the medium with each extraction or normal medium. From 1 day to 3 days, the cell viability and proliferation were the same for all groups, which means the dissolved silicon-containing species in the medium do not affect the cell adhesion to early cell division. From 3 days to 5 days, the cell proliferation was suppressed by ChG05 and ChD05, while ChT05 did not suppress proliferation.

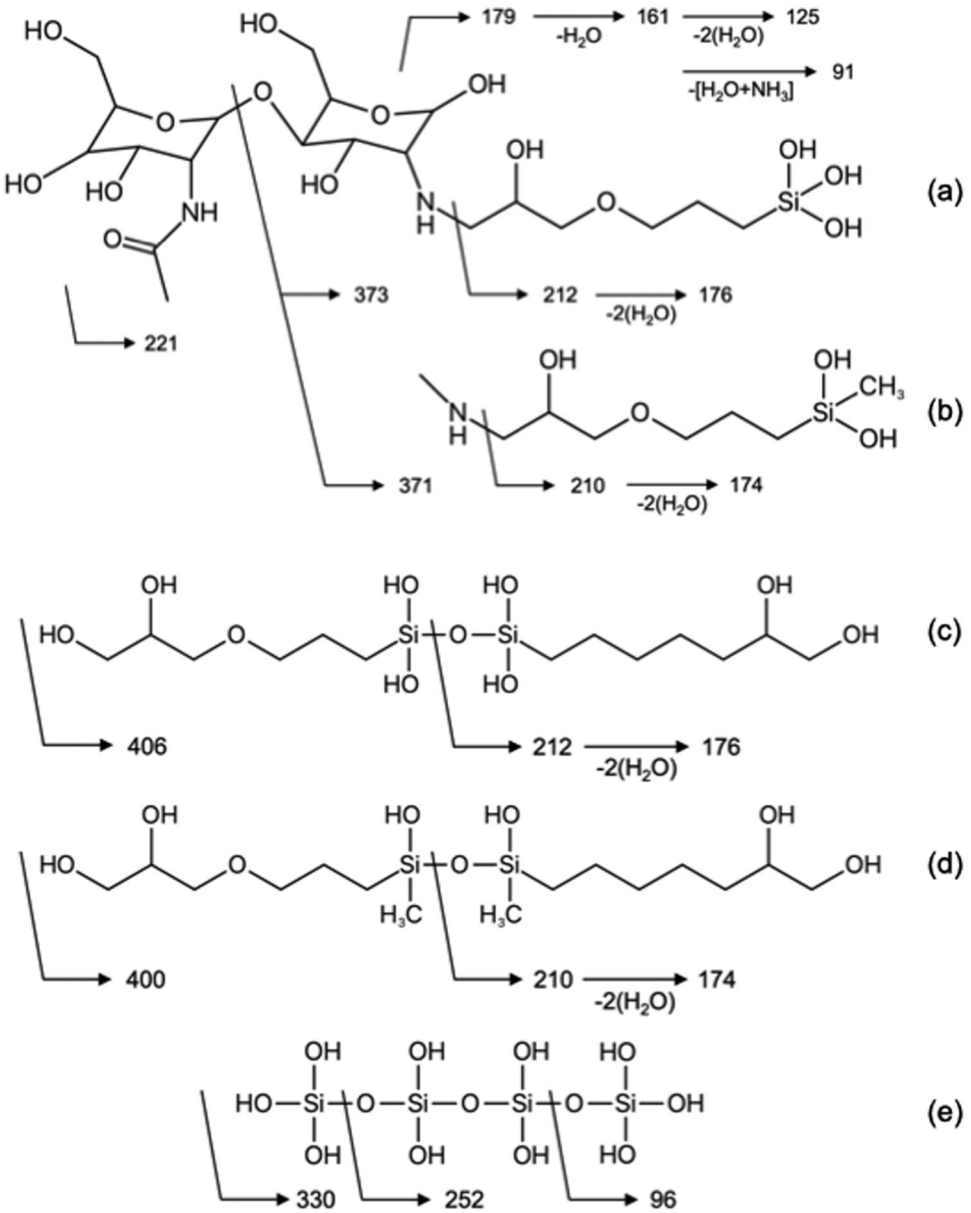

Fig. 5 Structure and the molecular weight of the dissolved product of (**a**, **c**) ChG05, (**b**, **d**) ChD05, and (**e**) ChT05 estimated from TOF-MS spectrum

Figures 7, 8, and 9 show RT4 cell morphologies at 1, 3, and 5 days culture, respectively. All RT4 nerve cells showed nearly the same morphologies with pseudopodia at 1 day and 3 days. After 5 days of culture, the RT4 cells showed a spindle-like shape in all cultures. In case of the osteoblast cell, the proliferation and differentiation were suppressed when the Si(IV) concentration in the medium was 6–8.19 mM [4, 5]. Compared with osteoblast cells, the proliferation of nerve cells was extremely inhibited at lower Si(IV) concentration, indicating that the effect of silicon depends on the cell type. Alternatively, chitosan oligomers with a polymerization degree of less than seven promote the proliferation of Schwann cells [32].

In this study, chitosan-derived molecules were detected in all extractions using TOF-MS; however, the proliferation was not improved. Chitosan-derived molecules were monomers; therefore, they did not impact the nerve cell proliferation. Both ChG05 and ChD05 inhibited nerve cell proliferation. The extraction of ChT05 contained the monomer of orthosilicic acid; however, the ChG05 and ChD05 extraction mainly contained monomeric species with organic chains of GPTMS or GPDMS, and chitosan. The organic chains bonded to silicon atoms impact only the proliferation of nerve cells. Figures 10 and 11 show the amount of intracellular Si(IV) and the Si(IV) concentration in the supernatant medium at 5 days culture, respectively. The amount of intracellular Si(IV) of ChD05 and ChT05 was the same as the control, with ChG05 having the least. In the case of ChG05, the Si(IV) concentration did not change from the initial concentration. Alternatively, in the

case of ChD05 and ChT05, the Si(IV) concentration slightly decreased.

Orthosilicate was taken up by osteoblast cells via sodium–bicarbonate ion channels (0.3 nm), promoting cell differentiation [6]. Obata et al. [33] reported that the Si(IV) component released from siloxane-doped calcium carbonate was not taken up by osteoblast cells at a concentration of 50 ppm. Alternatively, they reported that the Si(IV) component eluted from Bioglass® 45S5 was taken up by osteoblast cells at a concentration of 50 ppm. The species dissolved from our hybrids are similar to those from the siloxane-doped calcium carbonate and were not taken up by the nerve cells. In addition, Shie et al. observed the taken up of Si(IV) components in osteoblast cells by pinocytosis to form intracellular vacuoles [5]. In our results, changes in the amount of the intracellular Si(IV) and vacuoles were not observed in the fluorescence images, suggesting that the silicon-containing species were not taken up by the cells. The concentration of Si(IV) in the supernatant medium after incubation was nearly unchanged in ChG05, slightly decreasing in ChD05 and ChT05 from the initial concentration. Therefore, the silicon-containing species adsorb or desorb to the cell surface or the components such as proteins in the culture medium. Figure 12 concludes our assessment of the results. In the case of ChT05, the silicon-containing species were monomers or oligomers derived from TEOS and adsorbed to the cell surface; however, they did not affect cell proliferation. The silicon-containing species dissolved from ChD05 also adsorbed to the cell surface, but inhibited the cell proliferation. The species dissolved from ChG05 did not adsorb to the cell surface, but inhibited the cell proliferation. Therefore, the species dissolved from ChG05 inactivate the components for cell growth in the culture medium or disturb the ion exchange near the ion channel because the intracellular Si(IV) decreases. The inactivation of components is also possible for ChD05, indicating that the organic chains bonded to silicon atoms are involved in the adsorption to components for nerve cell growth.

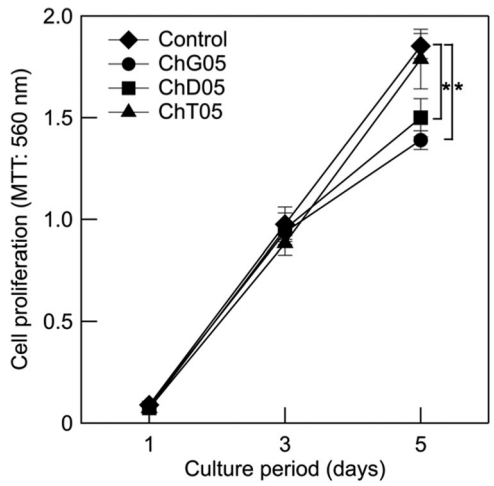

Fig. 6 Cell proliferation in the medium with different extractions. *$p <$ 0.01

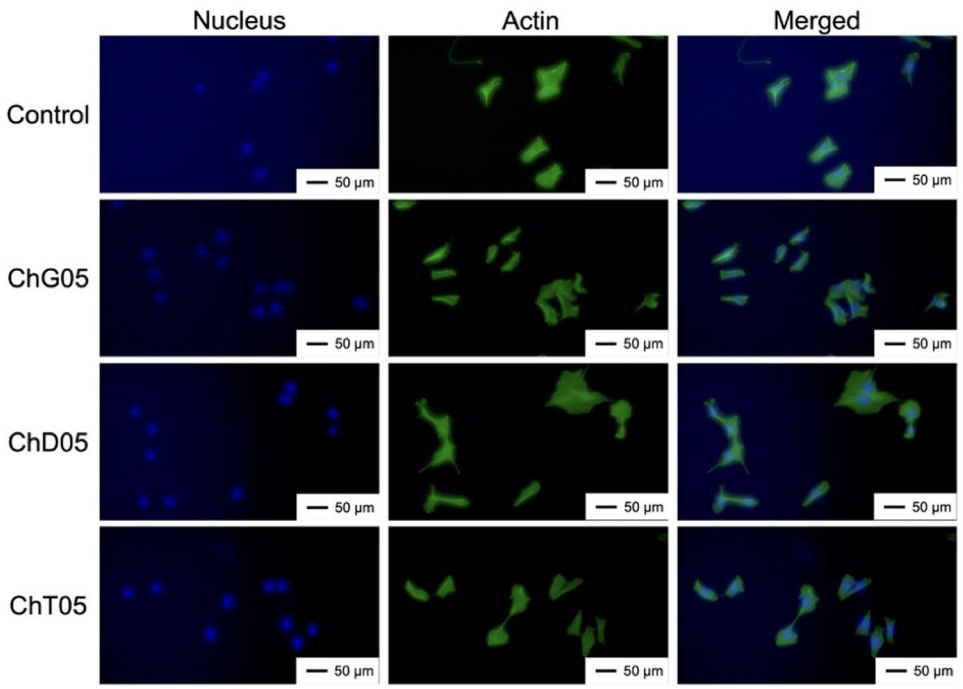

Fig. 7 Fluorescent image of RT4 cells cultured in the control, ChG05, ChD05, and ChT05 medium at 1 day

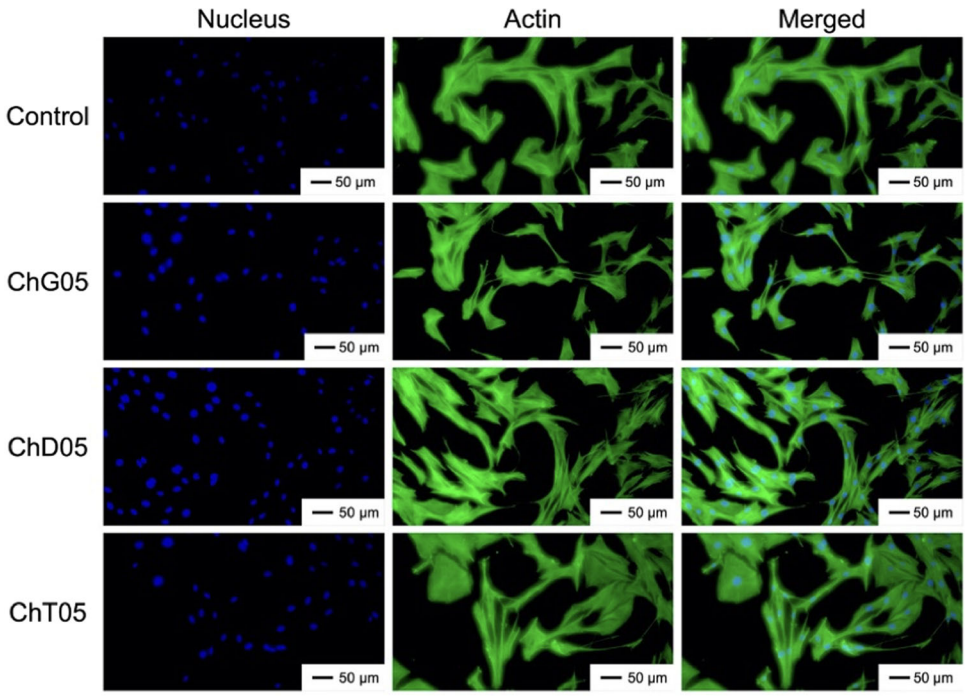

Fig. 8 Fluorescent image of RT4 cells cultured in the control, ChG05, ChD05, and ChT05 medium at 3 days

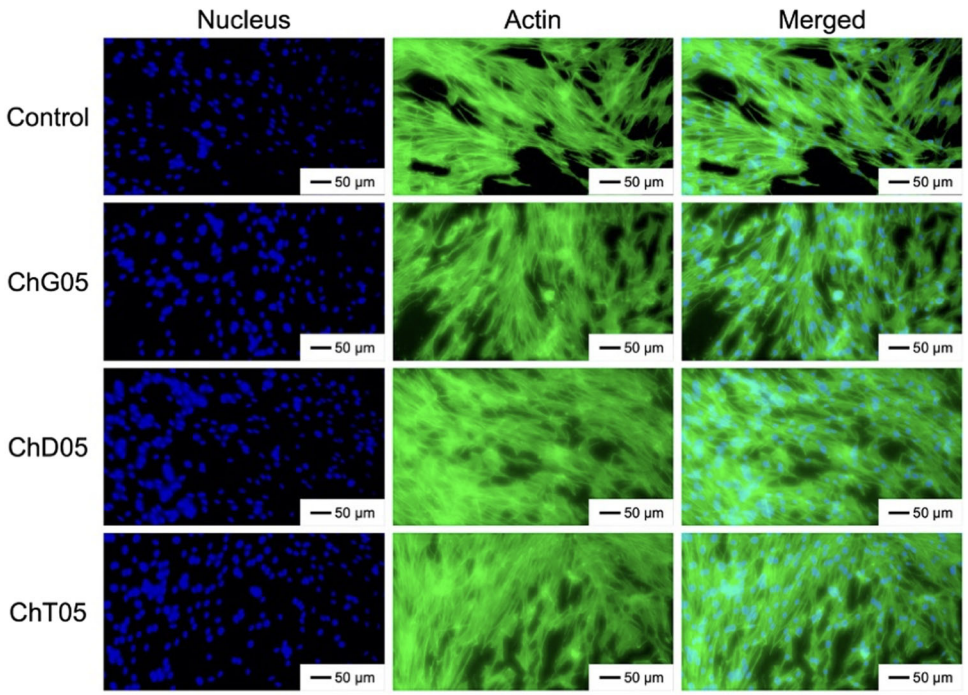

Fig. 9 Fluorescent image of RT4 cells cultured in the control, ChG05, ChD05, and ChT05 medium at 5 days

4 Conclusions

Chitosan- and chitin-derived degradation products were observed in all extracts and they were not involved in the inhibition of nerve cell proliferation. The 100–400 species dissolved from the hybrids in the extracts of ChG05 and ChD05 include monomeric silicon-containing species derived from GPTMS and GPDMS, which inhibited the cell proliferation. The silicon-containing species dissolved from ChT05 adsorbed to the cell surface, but did not affect cell proliferation. The silicon-containing species dissolved from ChD05 also adsorbed to the cell surface, but inhibited the cell proliferation. The species dissolved from ChG05 did not adsorb to the cell surface, but inhibited the cell proliferation. Therefore, the species dissolved from ChG05 inactivate the components for cell growth in the culture

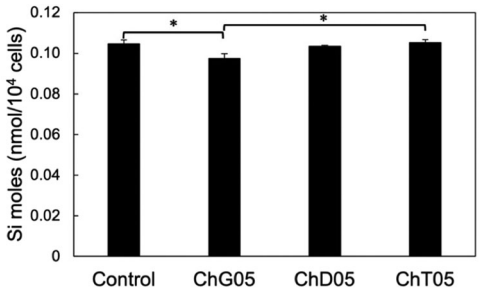

Fig. 10 The amount of intracellular Si(IV) at 5 days culture. $*p < 0.01$

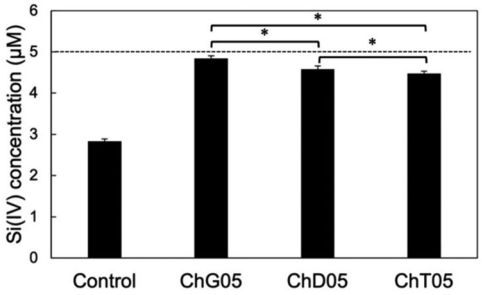

Fig. 11 Si(IV) concentration of supernatant medium at 5 days culture. $*p < 0.01$

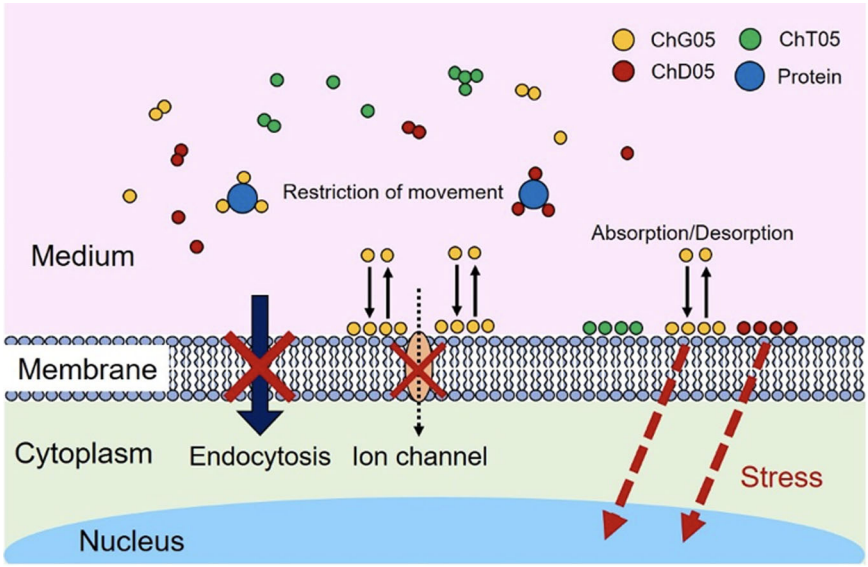

Fig. 12 The effect of the silicon-containing species dissolved from the chitosan–siloxane hybrid membranes on the nerve cell

medium or disturb the ion exchange near the ion channel because of the results of the intercellular Si(IV) decrease. The organic chains bonded to silicon atoms are involved in the adsorption of components for nerve cell growth.

Acknowledgements We gratefully acknowledge Masumi Kunisue, Center for Instrumental Analysis, Equipment Sharing Sector, Organization for Promotion of Open Innovation, Kyushu Institute of Technology, for TOF-MS measurement. We thank Ashleigh Cooper, PhD, from Edanz (https://jp.edanz.com/ac) for editing a draft of this manuscript.

Funding This research was supported by the Japan Society for the Promotion of Science (JSPS) KAKENHI (grant Number JP19H04471).

Compliance with ethical standards

Conflict of interest The authors declare no competing interests.

Publisher's note Springer Nature remains neutral with regard to jurisdictional claims in published maps and institutional affiliations.

References

1. Lansdown AB, Williams A (2007) A prospective analysis of the role of silicon in wound care. J Wound Care 16(9):404–407. https://doi.org/10.12968/jowc.2007.16.9.27865
2. Carlisle EM (1988) Silicon as a trace nutrient. Sci Total Environ 73(1–2):95–106. https://doi.org/10.1016/0048-9697(88)90190-8
3. Xynos ID, Edgar AJ, Buttery LDK, Hench LL, Polak JM (2000) Ionic products of bioactive glass dissolution increase proliferation of human osteoblasts and induce insulin-like growth factor II mRNA expression and protein synthesis. Biochem Biophys Res Commun 276(2):461–465. https://doi.org/10.1006/bbrc.2000.3503
4. Gough JE, Jones JR, Hench LL (2004) Nodule formation and mineralisation of human primary osteoblasts cultured on a porous bioactive glass scaffold. Biomaterials 25(11):2039–2046. https://doi.org/10.1016/j.biomaterials.2003.07.001
5. Shie MY, Ding SJ, Chang HC (2011) The role of silicon in osteoblast-like cell proliferation and apoptosis. Acta Biomater 7 (6):2604–2614. https://doi.org/10.1016/j.actbio.2011.02.023
6. Zhou X, Moussa FM, Mankoci S, Ustriyana P, Zhang N, Abdelmagid S, Molenda J, Murphy WL, Safadi FF, Sahai N (2016) Orthosilicic acid, Si(OH)4, stimulates osteoblast differentiation in vitro by upregulating miR-146a to antagonize NF-κB activation. Acta Biomater 39:192–202. https://doi.org/10.1016/j.actbio.2016.05.007

7. Kim KJ, Joe YA, Kim MK, Lee SJ, Ryu YH, Cho DW, Rhie JW (2015) Silica nanoparticles increase human adipose tissue-derived stem cell proliferation through ERK 1/2 activation. Int J Nanomed 10:2261–2272. https://doi.org/10.2147/IJN.S71925
8. Quignard S, Coradin T, Powell JJ, Jugdaohsingh R (2017) Silica nanoparticles as sources of silicic acid favoring wound healing in vitro. Colloids Surf B 155:530–537. https://doi.org/10.1016/j.colsurfb.2017.04.049
9. Fritsch-Decker S, An Z, Yan J, Hansjosten I, Al-Rawi M, Peravali R, Diabaté S, Weiss C (2019) Silica nanoparticles provoke cell death independent of p53 and BAX in human colon cancer cells. Nanomaterials 9(8):1172. https://doi.org/10.3390/nano9081172
10. Bonazza V, Borsani E, Buffoli B, Parolini S, Inchingolo F, Rezzani R, Rodella LF (2018) In vitro treatment with concentrated growth factors (CGF) and sodium orthosilicate positively affects cell renewal in three different human cell lines. Cell Biol Int 42 (3):353–364. https://doi.org/10.1002/cbin.1090
11. Shirosaki Y, Tsuru K, Moribayashi H, Hayakawa S, Nakamura Y, Gibson IR, Osaka A (2010) Preparation of osteocompatible Si (IV)-enriched chitosan-silicate hybrids. J Ceram Soc Jpn 119 (11):989–992. https://doi.org/10.2109/jcersj2.118.989
12. Teruo O, Masayuki Y (2007) In: Recent progress in Regenerative Medicine Technologies, Chapter 4 Soft Tissues. Tokyo, Japan
13. Gupta B, Papke JB, Mohammadkhah A, Day DE, Harkins AB (2016) Effects of chemically doped bioactive borate glass on neuron regrowth and regeneration. Ann Biomed Eng 44 (12):3468–3477. https://doi.org/10.1007/s10439-016-1689-0
14. Mobasseri SA, Terenghi G, Downes S (2013) Micro-structural geometry of thin films intended for the inner lumen of nerve conduits affects nerve repair. J Mater Sci: Mater Med 24 (7):1639–1647. https://doi.org/10.1007/s10856-013-4922-5
15. Jiang X, Lim SH, Mao Hai-Quan HQ, Chew SY (2010) Current applications and future perspectives of artificial nerve conduits. Exp Neurol 223(1):86–101. https://doi.org/10.1016/j.expneurol.2009.09.009
16. Boecker A, Daeschler SC, Kneser U, Harhaus L (2019) Relevance and recent developments of chitosan in peripheral nerve surgery. Front Cell Neurosci 13:104. https://doi.org/10.3389/fncel.2019.00104
17. Dietzmeyer N, Förthmann M, Grothe C, Haastert-Talini K (2020) Chitosan tubes prefilled with aligned fibrin nanofiber hydrogel enhance facial nerve regeneration in rabbits. ACS Omega 6:26293–26301. https://doi.org/10.4103/1673-5374.271668
18. Mu X, Sun X, Yang S, Pan S, Sun J, Niu Y, He L, Wang X (2021) Dog sciatic nerve regeneration across a 30-mm defect bridged by a chitosan/PGA artificial nerve graft. Brain 128(8):1897–1910. https://doi.org/10.1021/acsomega.1c03245
19. Amado S, Simões MJ, Armada da Silva PAS, Luís AL, Shirosaki Y, Lopes MA, Santos JD, Fregnan F, Gambarotta G, Raimondo S, Fornaro M, Veloso AP, Varejão ASP, Maurício AC, Geuna S (2008) Use of hybrid chitosan membranes and N1E-115 cells for promoting nerve regeneration in an axonotmesis rat model. Biomaterials 29(33):4409–4419. https://doi.org/10.1016/j.biomaterials.2008.07.043
20. Simões MJ, Amado S, Gärtner A, Armada da Silva PAS, Raimondo S, Vieira M, Luís AL, Shirosaki Y, Veloso AP, Santos JD, Varejão ASP, Geuna S, Maurício AC (2010) Use of chitosan scaffolds for repairing rat sciatic nerve defects. Ital J Anat Embryol 115(3):190–210. https://doi.org/10.13128/IJAE-9074
21. Simões MJ, Gärtner A, Shirosaki Y, Gil da Costa RM, Cortez PP, Gärtner F, Santos JD, Lopes MA, Veloso AP, Varejão ASP, Maurício AC (2011) In vitro and in vivo chitosan membranes testing for peripheral nerve reconstruction. Acta Med Port 24 (1):43–51. https://doi.org/10.20344/AMP.344
22. Shirosaki Y, Hayakawa S, Osaka A, Lopes MA, Santos JD, Geuna S, Maurício AC (2014) Challenging for nerve repair using chitosan-siloxane hybrid porous scaffolds. BioMed Res Int 153808. https://doi.org/10.1155/2014/153808
23. Berridge MV, Tan AS (1993) Characterization of the cellular reduction of 3-(4,5-dimethylthiazol-2-yl)-2,5-diphenyltetrazolium bromide (MTT): subcellular localization, substrate dependence, and involvement of mitochondrial electron transport in MTT reduction. Arch Biochem Biophys 303:474–482. https://doi.org/10.1006/abbi.1993.1311
24. Shirosaki Y, Hirai M, Hayakawa S, Fujii E, Lopes MA, Santos JD, Osaka A (2015) Preparation and in vitro cytocompatibility of chitosan-siloxane hybrid hydrogels. J Biomed Mater Res 103 (1):289–299. https://doi.org/10.1002/jbm.a.35171
25. Zhang M, Hisamori H, Yamada T, Hirano S (1994) 13C CP/MAS NMR spectral analysis of 6-O-tosyl, 6-deoxy-6-iodo, and 6-deoxy derivatives of N-acetylchitosan in a solid state. Biosci Biotech Biochem 58(10):1906–1908. https://doi.org/10.1271/bbb.58.1906
26. Davis RS, Brough AR, Atkinson A (2003) Formation of silica/epoxy hybrid network polymers. J Non-Cryst Solid 315:197–205. https://doi.org/10.1016/S0022-3093(02)01431-X
27. Kumamoto K, Maeda T, Hayakawa S, Mustapha NAB, Wang MJ, Shirosaki Y (2021) Antibacterial chitosan nanofiber thin films with bacitracin zinc salt. Polymers 13(7):1–15. https://doi.org/10.3390/polym13071104
28. Shirosaki Y, Tsuru K, Hayakawa S, Osaka A, Lopes MA, Santos JD, Costa MA, Fernandes MH (2009) Physical, chemical and in vitro biological profile of chitosan hybrid membrane as a function of organosiloxane concentration. Acta Biomater 5 (1):346–355. https://doi.org/10.1016/j.actbio.2008.07.022
29. Zhou J, Xu T, Wang X, Liu C, Liao X, Huang X, Shi B (2017) A low-cost and water resistant biomass adhesive derived from the hydrolysate of leather waste. RSC Adv 7(7):4024–4029. https://doi.org/10.1039/c6ra27132d
30. Chen S, Hayakawa S, Shirosaki Y, Fujii E, Kawabata K, Tsuru K, Osaka A (2009) Sol-gel synthesis and microstructure analysis of amino-modified hybrid silica nanoparticles from aminopropyltriethoxysilane and tetraethoxysilane. J Am Ceram Soc 92 (9):2074–2082. https://doi.org/10.1111/j.1551-2916.2009.03135.x
31. Liu XM, Maziarz EP, Heiler DJ, Grobe GL (2003) Comparative studies of poly(dimethyl siloxanes) using automated GPC-MALDI-TOF MS and on-line GPC-ESI-TOF MS. J Am Soc Mass Spectrom 14(3):195–202. https://doi.org/10.1016/S1044-0305(02)00908-X
32. Wang Y, Zhao Y, Sun C, Hu W, Zhao J, Li G, Zhang L, Liu M, Liu Y, Ding F, Yang Y, Gu X (2016) Chitosan degradation products promote nerve regeneration by stimulating Schwann Cell proliferation via miR-27a/FOXO1 axis. Mol Neurobiol 53 (1):28–39. https://doi.org/10.1007/s12035-014-8968-2
33. Obata A, Iwanaga N, Terada A, Jell G, Kasuga T (2017) Osteoblast-like cell responses to silicate ions released from 45S5-type bioactive glass and siloxane-doped vaterite. J Mater Sci 52 (15):8942–8956. https://doi.org/10.1007/s10853-017-1057-y